

Sensitivity of stratospheric Br_y to uncertainties in very short lived substance emissions and atmospheric transport

R. Schofield¹, S. Fueglistaler^{2,*}, I. Wohltmann¹, and M. Rex¹

¹Alfred Wegener Institute, Potsdam, Germany

²Department of Applied Mathematics and Theoretical Physics, University of Cambridge, Cambridge, UK

*now at: Department of Geosciences, Princeton University, New Jersey, USA

Received: 11 September 2010 – Published in Atmos. Chem. Phys. Discuss.: 18 October 2010

Revised: 21 January 2011 – Accepted: 9 February 2011 – Published: 16 February 2011

Abstract. We evaluate the sensitivity of Br_y entering the stratosphere with a simplified model that allows calculations over a wide parameter range for parameters that are currently poorly quantified. The model examines the transport process uncertainties in the source concentrations and lifetimes, in the convective parameterization and in the inorganic bromine washout process due to dehydration. Source concentrations at the surface and lifetimes were found to have a slight effect on the resultant Br_y (1 ppt), however this was highly dependent upon, with increasing significance, the BL component of convectively delivered air. Efficiency of convective delivery of boundary layer (BL) air to the tropical tropopause layer (TTL) along with washout at the CPT were found to substantially affect Br_y at 400 K – altering the delivered Br_y by 3.3 ppt and 2.9 ppt, respectively. We find that the results critically depend on free tropospheric bromine source gas concentrations due to dilution of convective updrafts, and the processes that control free tropospheric bromine source gas concentrations require further attention.

1 Introduction

Bromine was first proposed to play a key role in ozone destruction by Wofsy et al. (1975), and subsequently has been shown to be very efficient at both mid- and polar latitudes in the lower stratosphere (Dvortsov et al., 1999; Lee et al., 2002). However, the stratospheric bromine budget remains poorly quantified. Stratospheric measurements of BrO from ground-based, balloon and satellite platforms can only be explained with an additional 3–8 ppt of total reactive bromine (Br_y) to that provided by the long lived bromine containing halons and CH₃Br (Law and Sturges, 2007). The bromine

containing very short-lived substances (VSLS), with lifetimes less than 6 months, have been suggested to bridge this shortfall in the stratospheric bromine budget (Sinnhuber et al., 2002, 2005; Schofield et al., 2004, 2006; Salawitch et al., 2005; Dorf et al., 2006; Livesey et al., 2006; Hendrick et al., 2007; Theys et al., 2009; Sioris et al., 2006).

The transport of VSLS from their sources to the stratosphere is complex, and a model from emission at the surface to stratospheric Br_y that captures all intricacies is not yet realisable. In particular, the following processes have been identified as main sources of uncertainty:

- VSLS source concentrations:
the VSLS have predominantly natural sources, e.g. marine macro-algae. Questions remain about the conditions under which increased bromine VSLS are produced, and therefore which seasons and locations are “hot spots” for bromine VSLS production.
- VSLS lifetimes:
the lifetimes of the VSLS bromocarbons are determined by OH concentrations and photolysis. OH concentrations in the TTL are uncertain but likely lower than in the free troposphere, and consequently VSLS lifetimes may be longer.
- Transport from boundary layer (BL) to the tropical tropopause layer (TTL):
transport within the BL, and the entrainment of BL air into deep convective cells is not well constrained. The modelling of deep convective events is challenging: therefore capturing the timing, location and the proportion of BL air detraining into the TTL remains uncertain.
- Transport and washout in the TTL:
the transport time-scale in the TTL is similar to that of the lifetime of VSLS, such that washout of inorganic



Correspondence to: R. Schofield
(robbyn.schofield@awi.de)

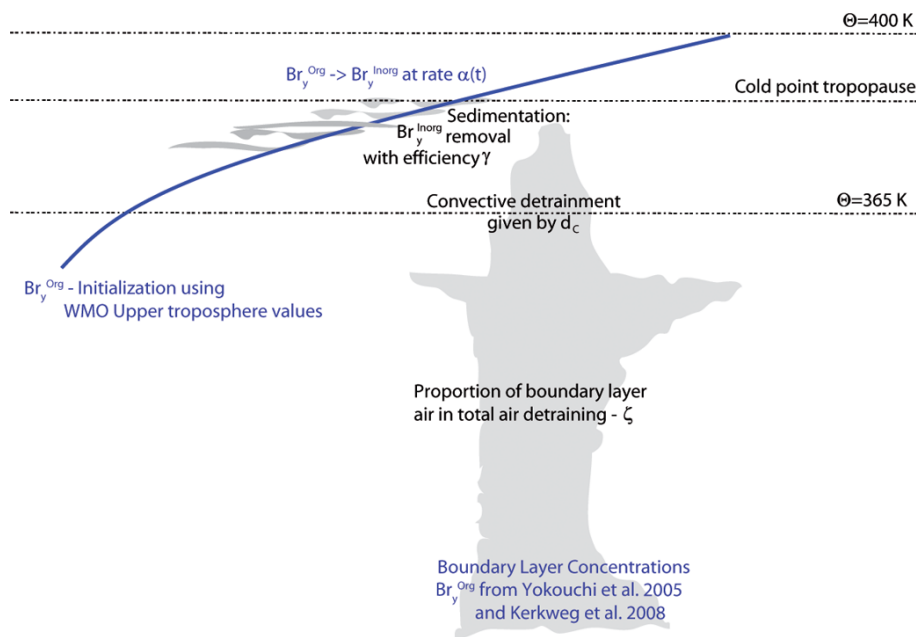


Fig. 1. Schematic illustration of the conceptualised model. The blue line is a single trajectory depicting a “typical” air parcel traversing 365–400 K. Each air parcel trajectory experiences convective injection of organic bromine delivered from the BL and the FT (with the BL component given by ζ between 0 and 1). From t_0 inorganic bromine from SLS loss forms at an overall rate given by α , determined cumulatively from all of SLS bromine species’ lifetimes. As the air parcel dehydrates at cold temperatures, the available inorganic bromine washes out with an efficiency γ (between 0 and 1). After the CPT is crossed possible introduction of additional organic bromine via convection contributes to the total amount of bromine reaching 400 K.

product species during dehydration in the TTL may remove a substantial fraction of Br_y.

Our study seeks to quantify the relative importance of the (large) uncertainties in each of these steps. We use a lagrangian model with trajectories based on data from the European Centre for Medium-range Weather Forecasts (ECMWF) ERA-Interim data (Simmons et al., 2007) as representation of the global circulation in combination with a simplified representation of the processes affecting VLSL concentrations during transport from troposphere to stratosphere. For each process, the model has a “tuning knob” that allows evaluation of sensitivities. In Sect. 2 the conceptual model setup describing the simplified microphysical and VLSL box model is outlined. In Sect. 3 we discuss the sensitivities of the resultant stratospheric Br_y budget to the conceptualized chemical, microphysical and convective processes that control the stratospheric bromine budget.

2 Conceptual model set-up

We use the following conceptual model to estimate the total bromine concentration of air entering the stratospheric overworld (i.e. above 380 K potential temperature, Hoskins, 1991). Trajectories based on data from ERA-Interim are used as the representation of the large-scale circulation. A simple

process “box model” is run along the trajectory to represent the effect of deep convection detraining into the TTL, and to calculate the effect of chemical and washout processes on Br_y delivery to the stratosphere. Trajectories are started on 28/2 (DJF), 31/5 (MAM), 31/8 (JJA) and 30/11 (SON) for 2000 through 2005 at 400 K on a 2° latitude × 2° longitude grid between 50° N and 50° S. They are traced backwards in time using the analysed horizontal wind fields and the clear-sky radiative heating rates obtained from the ERA-Interim forecast runs. Trajectories are calculated with a 10 min integration timestep and are saved with a 30 min timestep. Further details of the trajectory model are given by Wohltmann and Rex (2008).

Figure 1 provides a simple pictorial view of the processes controlling the delivery of bromine to the stratosphere. The thick blue line illustrates a 3 month back-trajectory started at 400 K that crosses $\Theta=365$ K. Only trajectories that have crossed 365 K during the 3 months are considered in this study – this is 71% of the trajectories in DJF 2000 and 66% in JJA 2000. At t_0 , the earliest time of the back trajectory, Br_y^{OrgSL} (the mixing ratio total of bromine atoms in the organic short lived bromine substances or source gases (SG) – χ^{SG}) is initialized with the WMO 2006 recommendations for the upper troposphere (UT) (Law and Sturges, 2007, Table 2–2):

$$\chi^{\text{SG}} = \text{CH}_3\text{Br} + 2\text{CH}_2\text{Br}_2 + 3\text{CHBr}_3 + 2\text{CHBr}_2\text{Cl} + \text{CH}_2\text{BrCl} + \text{CHBrCl}_2 \quad (1)$$

As the trajectory ascends the TTL χ^{SG} is increased by convection (see Sect. 2.2 below) which transports a mixture of boundary-layer and free-tropospheric air with corresponding SLS concentrations. The proportion of the detrained air of BL origin is given by the efficiency parameter ζ (see Sect. 2.3). ζ is allowed to vary between 0 (no BL organic bromine containing species in convective outflow) to 1 (BL bromine species detrain undiluted). The Br_y^{OrgSL} SGs are converted to highly soluble product gases (PGs); Br_y^{Inorg}, at a rate that is determined by α . α is derived from the individual SG lifetimes and is suitably adjusted when convective injection of “younger air” occurs (see Sect. 2.4). Br_y^{Inorg} is a catch all for the product species of bromocarbon breakdown, thought to be dominated by HOBr and HBr (85%) in the TTL region, the rest made up from Br₂ and BrO (Fig. 4 from Yang et al., 2005). The highly soluble Br_y^{Inorg} is accumulated along the trajectory and partly removed from the system at the time of the last dehydration at the trajectory’s cold point. The parameter γ determines the efficiency of this washout, with values between 0 (complete retention of the PG) to 1 (complete PG removal at the cold point) as detailed in Sect. 2.5.

2.1 Br_y source budget

The bromine containing VLSLs with lifetimes from 3.5 weeks to 5 months, and methyl bromide with a longer lifetime of 0.7 years are all the species that are thought to contribute to the tropospheric (Yang et al., 2005), hence TTL reactive bromine budget. All of these bromocarbons, along with the long lived halons and the number of bromine atoms they contribute are listed in Table 1 and make up the known and potential stratospheric Br_y budget. The VLSL bromocarbons have known oceanic sources from ice algae, macroalgae and phytoplankton, whereas CH₃Br has both natural (oceanic) and anthropogenic (fumigation and biomass burning) sources (Yang et al., 2005).

In the first emission scenario given in Table 2 both oceanic and coastal boundary layer concentrations of CH₂Br₂, CHBr₃ and CHBr₂Cl are prescribed from the (purposely selected) high measurements of Yokouchi et al. (2005). The land values are those given by WMO (2006). An alternative second BL source scenario based upon Kerkweg et al. (2008) has 4 times less CHBr₃ in the coastal BL and slightly less CH₂Br₂. In this second scenario the most abundant tropospheric bromine containing species, CH₃Br is increased to 10 ppt, typical of 30° N with no coastal/oceanic or land differences. The first scenario tests the influence of very high oceanic and coastal CHBr₃ and CH₂Br₂ concentrations, and the second scenario lower VLSL values – but more CH₃Br with a longer lifetime – emulating a longer-lived SLS sce-

Table 1. Br_y contributing organic source gases initialized for the base of the TTL $\Theta = 365$ K. Halons and CH₃Br as prescribed from WMO (2006, Table 8–5) for year 2000 and VLSL species as given by the upper limit of the observed range (WMO, 2006, Table 2–2). Lifetimes from WMO (2006, Table 1–4).

Species	UT Conc [ppt]	Lifetime [yr (days)]	Number Br atoms
Halon1301	2.71	65	1
Halon1211	4.01	16	1
Halon2402	0.41	20	2
Halon1202	0.05	2.9	2
CH ₃ Br	8.90	0.7 (256)	1
CH ₂ Br ₂	1.0	0.33 (120)	2
CHBr ₃	0.7	0.07 (26)	3
CHBr ₂ Cl	0.12	0.19 (69)	2
CH ₂ BrCl	0.35	0.41 (150)	1
CHBrCl ₂	0.15	0.21 (78)	1

nario. These scenarios do not test the emission extremes; the lowermost extreme is similar to considering less convective influence. Therefore these two scenarios are representative examples and don’t encompass the entire range of observed values: for example, Carpenter et al. (2009) observed mean oceanic and coastal values of 0.3 and 3.3 ppt for CHBr₃ respectively and 0.3 and 1.1 ppt for CH₂Br₂ – so lower than the Kerkweg et al. (2008) scenario. Similarly, much higher levels of CH₃Br – up to 60 ppt – have been observed and associated with biomass burning (Andreae et al., 1996). While the scenarios tested here go some way to quantifying the sensitivity of stratospheric Br_y to source strength and lifetime questions, a complete study will take into account fully the geographical patterns and photochemical lifetimes.

Figure 2 displays the SG contribution of each of the species to the stratospheric Br_y budget (Br_y^{OrgSL} + Br_y^{Halons}) for the two emission scenarios and its decay with time from the initial time of t_0 . The WMO recommendations (Law and Sturges, 2007) for the UT background concentration is shown in the top left panel of Fig. 2. The second and third left hand panels show oceanic and coastal concentrations of the Br_y^{OrgSL} (with decay over time) for the Yokouchi et al. (2005) emission scenario (refer to Table 2). The right hand panels result from the second emission scenario and altered lifetime based on Kerkweg et al. (2008) also provided in Table 2. The coastal regions which display the highest Br_y^{OrgSL} are defined as 2° latitude × 2° longitude boxes containing both land and ocean.

2.2 Convective mixing

By construction, the pathways of the trajectories do not include vertical transport from convection, as this is a sub-grid process and no latent heat release is included in the diabatic

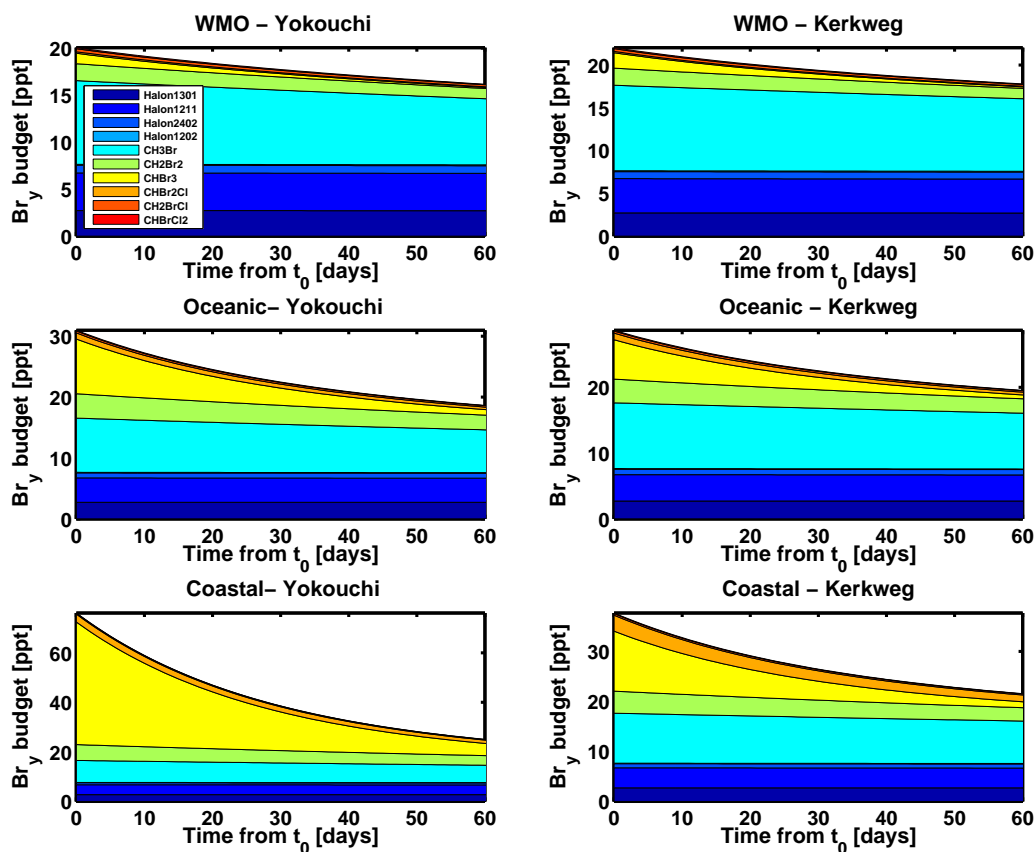


Fig. 2. The source gas contributions of bromine containing substances to the stratospheric Br_y budget from t_0 (entrance time in the TTL). Both of the scenarios given in Table 2 are provided. The VLSL concentrations for the upper troposphere as provided in the WMO report (Law and Sturges, 2007) (upper left) and with the adjustment of CH₃Br for the Kerkweg et al. (2008) scenario (upper right). The middle and lower panels give the oceanic and coastal concentrations for the VLSL respectively, for Yokouchi et al. (2005) (left) and Kerkweg et al. (2008) (right).

Table 2. SLS emission mixing ratio concentrations in the BL component of the convective outflow and the total Br_y contributed. Scenario 1 is based on Yokouchi et al. (2005) and scenario 2 upon Kerkweg et al. (2008).

	Yokouchi et al. (2005)				Kerkweg et al. (2008)			
	Land [ppt]	Coast [ppt]	Ocean [ppt]	τ [yr]	Land [ppt]	Coast [ppt]	Ocean [ppt]	τ [yr]
CH ₃ Br	8.90 ^a	8.90 ^a	8.90 ^a	0.7 ^b	10.0 ^d	10.0 ^d	10.0 ^d	1.0 ^e
CH ₂ Br ₂ ^b	0.9 ^a	3.2 ^c	2.0 ^c	0.33	1.0 ^d	2.2 ^d	1.8 ^d	0.33
CHBr ₃ ^b	0.37 ^a	16.5 ^c	3.0 ^c	0.07	0.6 ^d	4.0 ^d	2.0 ^d	0.07
CHBr ₂ Cl ^b	0.08 ^a	1.6 ^c	0.5 ^c	0.19	0.08 ^a	1.6 ^c	0.5 ^c	0.19
CH ₂ BrCl ^{a,b}	0.32	0.32	0.32	0.41	0.32	0.32	0.32	0.41
CHBrCl ₂ ^{a,b}	0.12	0.12	0.12	0.21	0.12	0.12	0.12	0.21
Total Br _y – SLS	12.4	68.4	23.3		14.4	30.0	21.0	
– VLSL	3.5	59.5	14.4		4.4	20.0	11.0	

^aConcentrations from WMO (2006) mean values, CH₃Br from Table 8–5 (year 2000) and VLSL from Table 2–2. ^bMid-tropospheric lifetimes from WMO (2006) table 1–4.

^cConcentrations from Yokouchi et al. (2005); coastal values from table 1 averaging sites S1, C1 and C2 and oceanic values from introductory text. ^dConcentrations from Kerkweg et al. (2008) Figs. 3, 5 and 16. ^eLifetime increased to 1.0 as found in Kerkweg et al. (2008) – 386 days (i.e. 1.06 years) and Montzka et al. (2003) \gg 0.8 years.

rates that are used to derive the vertical transport. Rather, the impact of convection is modeled by explicit mixing with convective air, for which we use the archived 3 hourly ERA-Interim detrainment rates (this calculation is performed offline from the trajectory code, and hence with the timestep given by the trajectory output, i.e. 30 min). Whenever a convective detrainment rate larger than zero is encountered, a fraction of the trajectory's "airmass" is replaced by convectively detrained air. The path of the trajectory prior to this mixing event can then be thought as being the path of the airmass into which the detrainment has occurred. We express this formally as follows. The fractional change in airmass characteristics, expressed in terms of VLS source gas (SG) mixing ratio χ^{SG} , is given by

$$\chi_i^{SG} = (d_c \times \Delta t) \chi_C^{SG} + (1 - d_c \times \Delta t) \chi_{i-1}^{SG} \quad (2)$$

where i denotes the iteration step, Δt is the model timestep, d_c is the detrainment rate provided as the archived parameter updraft detrainment from ECMWF (2008) (see Fig. 3), χ_{i-1}^{SG} is the mixing ratio of the SG (organic Br_y) on the trajectory prior to the mixing event, and χ_C is the mixing ratio of the convective outflow. Correspondingly, convective dilution of the product gas (PG: here Br_y^{Inorg}) is calculated by replacing SG with PG in the equation above, however, as no PG is assumed in the convective outflow, χ_C^{PG} is set to zero.

d_c , the detrainment rate is defined by ECMWF (2008):

$$d_c = \delta_{up} \times \frac{M_{up}}{\bar{\rho}} \quad (3)$$

where δ_{up} is the fractional detrainment (inversely proportional to the cloud radii), set to $0.94 \times 10^{-4} [\text{m}^{-1}]$ for deep convective clouds, M_{up} is the updraft mass flux and $\bar{\rho}$ the air density.

Figure 3 displays the 20° N to 20° S zonal mean seasonal profiles of the detrainment rates for 2000 used in this paper. Also displayed are the profiles for the three source regions for the DJF season, with the other seasons displaying almost identical behaviour. Both the coastal and land convection provide stronger detrainment up to 400 K compared to the mean oceanic convection. Within the 20° N to 20° S latitude range 8% is designated coastal, 21% land and 71% oceanic, thus the mean profile is dominated by oceanic convection. Tost et al. (2010) examining uncertainties arising from model convection schemes, including that of ECMWF, found while convective activity within the models studied was often poorly correlated with actual observed events, over longer timescales good agreement was achieved, that is longer-lived CO and O₃ UT concentrations were well modeled but shorter-lived species were not. Aschmann et al. (2009) found the ERA-Interim derived tropical mean turnover time compared very well with estimates from Dessler (2002) – providing further evidence that at least for averages over long time periods and long-lived species, the ERA-Interim detrainment rates perform well. Conversely,

however Folkins et al. (2006) argue for a pronounced annual cycle in deep convective detrainment based on ozone measurements, which is clearly not observed here. Therefore, the ERA-Interim detrainment rates provide a convenient, high temporal and spatial resolution measure of convective detrainment, but it has to be kept in mind, that they have an inherent uncertainty that is difficult to quantify.

Figure 4 shows the evolution of airmass along an example trajectory. Note how each mixing event reduces the importance of the characteristics prior to the mixing event – i.e. the system "loses memory". The loss of memory intrinsic to the system studied here reduces the sensitivity of results to the arguably somewhat ad-hoc initialisation in the upper troposphere. Indeed, results become more sensitive to the characteristics of the in-mixed air, a point we further discuss in Sect. 2.3 below. Generally, we find that in our model calculations convective in-mixing occurs prior to the trajectory's cold point, with only one or two weak events after the cold point (The example shown in Fig. 4 shows a case of several convective mixing events prior to, and one event after, the cold point.).

The approach chosen here to include the effect of convective in-mixing along a trajectory may be compared to the method of James et al. (2008). The key difference is that here, an individual trajectory eventually represents a spectrum of different convective origin, whereas their approach assigns each trajectory to one single convective event. We find that typically the spectrum of origin is dominated by the contributions from one or two convective events, which can be interpreted as the "most likely point of origin" equivalent to the single event scenario of James et al. (2008). The main difference for the calculation of Br_y of the two approaches arises from the non-linearity of the washout (see below) of inorganic product species, but the impact is less important than, for example, for the modelling of water isotopologues (Dessler et al., 2007) where the two methods yield quite different results (data not shown).

2.3 Convective dilution of BL air (ζ)

The VLS concentration of the convective outflow is a function of time and position of the convective mixing event. We assume that the convective detrainment represents a mixture of air directly from the boundary layer and entrained free tropospheric air, following the study of Romps and Kuang (2010) who found convective outflow only to comprise of between 10 and 30% of BL air. For the BL, we set χ_{BL} for land, coastal and oceanic sources either from Yokouchi et al. (2005) or Kerkweg et al. (2008) (see Table 2). For the free troposphere (FT), (χ_{FT}) we use the UT values recommended by Law and Sturges (2007). The dilution of fresh boundary layer air χ_{BL} by free tropospheric air χ_{FT} in the convective outflow χ_C is determined by a parameter ζ (ranging from 0

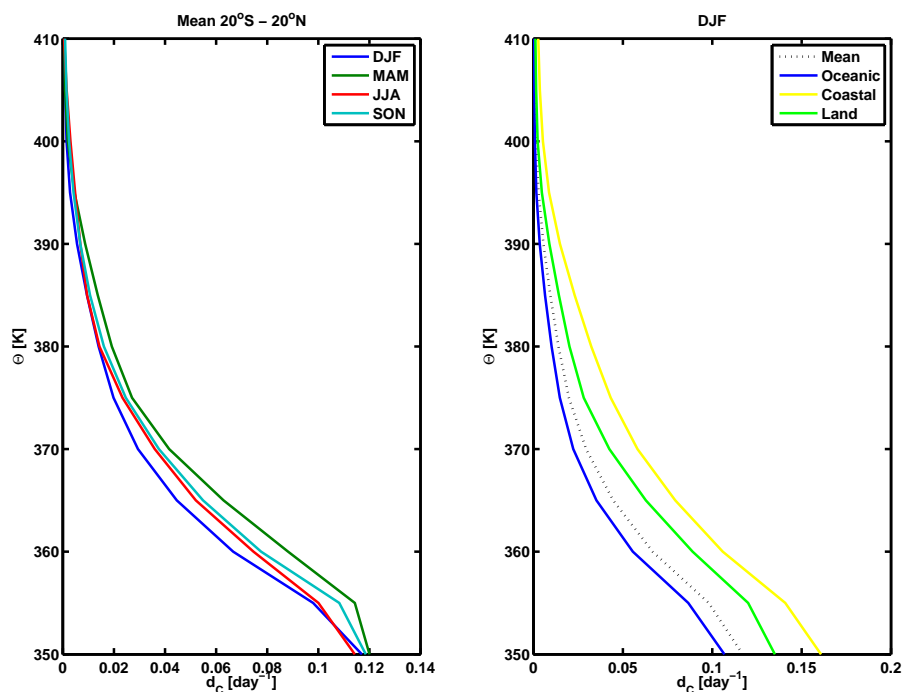


Fig. 3. 20° S–20° N zonal mean profiles of ERA-Interim detrainment rates for the seasons in 2000 (left) and source regions for DJF 2000 (right). Other years (and seasons) produce similar results.

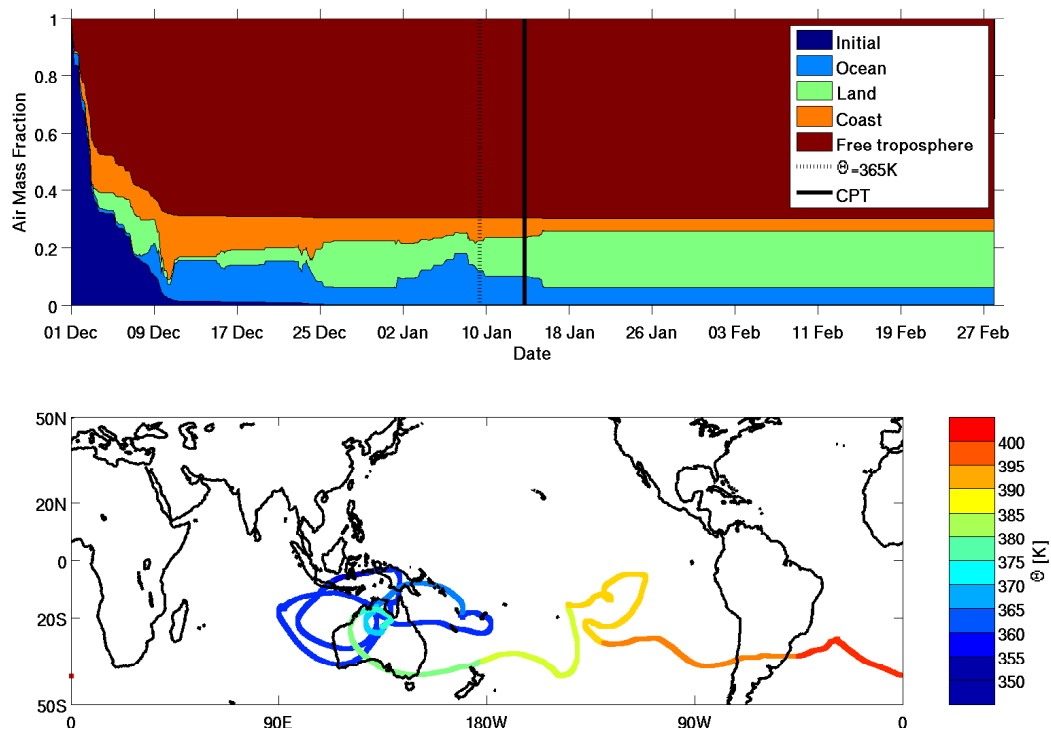


Fig. 4. How convection alters the air mass origin for a trajectory in DJF, 2000 is displayed in the upper panel (ζ , the BL component of convective outflow is set at 30%). Where $\Theta=365$ K and the CPT occur are indicated with the dashed and solid lines, respectively. The lower panel maps the trajectory path, with the colour designating the potential temperature of the trajectory.

to 1), such that

$$\chi_C = \zeta \chi_{BL}(\phi, \lambda) + (1 - \zeta) \chi_{FT} \quad (4)$$

Through variations in ζ we can determine the sensitivity to efficiency of convection to bring BL air directly into the TTL.

The χ_{BL} is assigned to be land, oceanic or coastal in nature, depending upon the location (latitude ϕ and longitude λ) of the trajectory for that timestep (see Fig. 4). Rather than tracking each species' contribution, we keep track of the average age of air and the fraction that comes from land, ocean, coastal or free tropospheric source regions. As pointed out before, for the situation where convective in-mixing is strong, the composition of the air mass eventually entering the stratosphere depends strongly on the characteristics of the “convective” air mass. Since we use the same “free tropospheric” concentrations for convection over land, coast and ocean, the “free tropospheric” concentrations approaches $1 - \zeta$ in this limit. This is evident in Fig. 4, where we have used $\zeta = 0.3$. Upon reaching a contribution of $1 - \zeta$ for free tropospheric air, subsequent convection can only change the partitioning between land, coast and ocean for the fraction ζ .

2.4 Br_y chemical lifetime (α)

The rate at which Br_y^{OrgSL} is converted to Br_y^{Inorg} is simplified in this work by introducing a single lifetime parameter α . The individual bromine source species are not accounted for separately, only the total organic short lived SGs: Br_y^{OrgSL} and their total degradation PGs (Br_y^{Inorg}) are saved along the trajectories, therefore an “overall” lifetime of Br_y^{OrgSL} that varies with convection is necessary. The individual species' lifetimes used in this work are given in Table 1 (Law and Sturges, 2007), e.g. for bromoform the lifetime is 26 days, which is in the middle of the range 15 to 37 days given by Warwick et al. (2006). α is the effective lifetime controlling the PG formation rate and is defined here as a concentration weighted lifetime for all the bromine species that have lifetimes shorter than one year (VSLs + CH₃Br). Note that CH₃Br is usually treated as a long lived species i.e. possible degradation in the TTL is not usually accounted for, however there is some loss of CH₃Br to inorganic bromine after only 15 days, the time required for ~80% of ascending trajectories to reach the cold point from 365 K and ~0.5 ppt CH₃Br to decay to PGs (see Fig. 2). This could lead to the underestimation of the Br_y deficit in the stratospheric bromine budget that needs to be explained by the VSLs.

The effective age of air upon the trajectory (t') is altered over an iteration as:

$$t'_i = t'_{i-1} \left(1 - \frac{(d_c \Delta t) \chi_C^{SG}}{\chi_i^{SG}} \right) + t'_c \left(\frac{(d_c \Delta t) \chi_C^{SG}}{\chi_i^{SG}} \right) + \Delta t \quad (5)$$

where t'_c is the age of the convectively introduced air (i.e. is zero), therefore the second term is zero. The fractional term in the above equation represents the proportion of VSLs

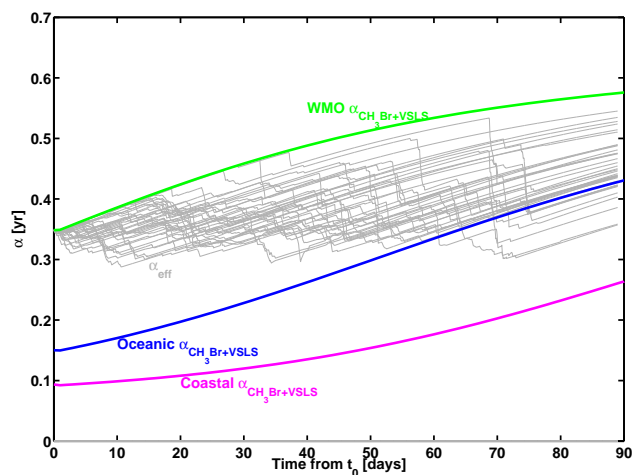


Fig. 5. The cumulative lifetime (α) in years of the short-lived bromine substances for the WMO upper troposphere (green), oceanic (blue) and coastal (magenta) regions from the concentration curves displayed in Fig. 2. Displayed in light grey is 50 example trajectories with their respective cumulative lifetimes – showing how convection from different source regions changes the α values (as the VSLs composition changes).

in the trajectory air parcel that was newly introduced by convection. When no convection occurs (i.e. $\chi_C^{SG} = 0$) then $t'_i = t'_{i-1} + \Delta t$ and the air parcel simply ages as expected by the model timestep.

The fraction of air (f) from each source region (land, ocean, coastal and free troposphere) is altered with each convective event and the cumulative lifetime is generated using the age of air and these fractions:

$$\alpha_i = \sum_{j=1}^n f_j \times \alpha_j(t') \quad (6)$$

where n is the number of source regions (here 4) and $\alpha(t')$ is the cumulative lifetime for the age of air of the air parcel.

The lifetimes used in this work are for mid-troposphere, so the TTL lifetimes are very likely to be different from these. We expect that lower OH concentrations in the TTL will outweigh the increased photolysis and thereby increase the lifetimes (especially that of CH₂Br₂ which undergoes little photolytic loss, Hossaini et al., 2010). We explore the effect of increasing the lifetime of CH₃Br as this is the most abundant SG in the second emission scenario run.

α can be viewed as the e-folding lifetime (Gettelman et al., 2009) determining the PG formation rate via SG loss. The formation of PG is given over a timestep by:

$$\chi_i^{PG} = \chi_{i-1}^{PG} + \frac{\chi_{i-1}^{SG}}{\alpha_i} \Delta t \quad (7)$$

where $\Delta t = t_i - t_{i-1}$ is the model timestep. The second term of the right hand side of Eq. (7) represents the loss of the SG

to PG; thereby the complementary equation for the degradation of the SG is given as:

$$\chi_i^{SG} = \chi_{i-1}^{SG} - \frac{\chi_{i-1}^{SG}}{\alpha_i} \Delta t \quad (8)$$

α changes (following Eq. 6) as the contributions from different sources via convection, alters the individual species' concentrations, as demonstrated in Fig. 5 by the example trajectories. Convective injection tends to decrease the cumulative lifetime by introducing short-lived substances: after 40 days the initial UT Br_y cumulative lifetime would be 0.4 yr (~150 days) without convective influence, through convection this is reduced to 0.2 yr (~73 days) with $\zeta = 30\%$ (see Sect. 2.3).

2.5 Washout of inorganic product species (γ)

Br_y^{Inorg} PG washout within the TTL is accounted for by introducing a parameter γ . As air ascends through the tropical tropopause almost all of the water condenses and is removed. Wet deposition of Br_y^{Inorg} is the largest removal mechanism for bromine containing substances. The question of how the soluble Br_y^{Inorg} interacts with the ice particles is a topic of current research, very relevant for both convective delivery/washout and advective ascent washout. The heterogeneous recycling of Br_y^{Inorg} into insoluble reactive forms has been demonstrated to increase the aerosol/cloud washout times from 6–9 days to 9–15 days at altitudes above 500 hPa (von Glasow et al., 2004). To investigate the relative importance of microphysics within the TTL the term γ varies between 0 and 1 to represent the fraction of soluble PG (Br_y^{Inorg}) that is simply removed at the CPT:

$$\chi_{CPT}^{Tot} = \chi_{CPT}^{SG} + (1 - \gamma) \times \chi_{CPT}^{PG} \quad (9)$$

where χ_{CPT}^{Tot} is the total bromine (Br_y) that survives washout at the CPT, thereby is guaranteed to enter the stratosphere, with only convective input above the CPT increasing this amount. Therefore, γ captures both the uptake efficiency of the aerosol/cloud particles and the heterogeneous recycling to insoluble bromine substances through the TTL. When $\gamma=0$ then there is no removal with ice sedimentation at the CPT and the total Br_y (Inorg+Org) that reaches 400 K is just the initialization value altered by convectively introduced χ_C^{SG} .

3 Discussion

In the following section the effective age of air reaching the CPT, the residence times (Fig. 6) and general properties of TTL transport provided by the back trajectories initiated at 400 K for the four seasons in 2000 are discussed. This is followed by a discussion of the Br_y transport sensitivity tests that look at the role of the sources, convection and washout upon the Br_y arriving at 400 K.

Figure 7 displays spatial distribution of Br_y arriving at 400 K for DJF and JJA in year 2000 using ERA-Interim detrainment rates as the convection proxy, BL concentrations defined by Yokouchi et al. (2005), a BL to outflow efficiency of 30% and complete CPT washout. Figure 8 provides the distribution of Br_y over all trajectories that ascend through the TTL 365–400 K, and arrive between 50° N and 50° S, at different stages of transport through the TTL. DJF with convection introducing a 30% BL component is displayed.

Figure 9 displays varying distributions highlighting the sensitivity of the results to season, washout, BL to outflow efficiency, convection after the CPT and source concentrations/lifetimes. Figure 10 displays the seasonal and inter-annual variation in the Br_y distribution being delivered to 400 K from 2000–2005. For the multiyear runs the UT initialization of Halons and CH₃Br decrease as prescribed in (WMO, 2006), otherwise the emissions of Yokouchi et al. (2005), ERA-Interim detrainment rates, ζ of 30%, and complete washout of Br_y^{Inorg} at the CPT, are used.

3.1 Residence times

The role of chemical conversion into soluble Br_y^{Inorg} and hence the role of washout on the water soluble Br_y^{Inorg} entering the stratosphere is critically dependent upon the time spent ascending through the TTL and the time since the last convective event. Following Eq. 5, the left panels of Fig. 6 display the effective convection corrected age of air reaching the CPT for each season in 2000. The effect of recent convective activity in reducing the effective age is clear. In the boreal winter greater air ages are associated with CPTs north of 10° N and conversely in boreal summer with CPTs south of 10° S. These patterns are anticipated following the seasonal shift of the convective inter-tropical convergence zone (ITCZ) (Fueglistaler et al., 2009).

The right-hand panels of Fig. 6 display the total transit time (residence time) from 365 to 400 K for each season. Also shown is the trajectory location at 355 K (open circles – nominal TTL “entry point”) for all trajectories that reach 400 K with residence times less than 30 days. The TTL entry points for the fastest TTL transport aggregate over the Western Pacific/Indonesia region, but a significant proportion also originate from the Indian Ocean and East Africa. This general picture holds for all years from 2000 to 2005. Note that no fast <30 day transits are seen for JJA.

The total transport times from 365 K to 400 K (Fig. 6) show a seasonal dependence with mean values of 45 days in DJF increasing to ~60 days in JJA, this is in qualitative agreement with the age of air at 17 km reported by Folkins et al. (2006) of 40 days for boreal winter (DJF) and 70 days for boreal summer (JJA). These residence times are significantly longer than trajectory study of Fueglistaler et al. (2004) using the too rapid vertical winds of ERA-40 which gave a seasonally independent transport time between 340 K and 400 K of about 30 days.

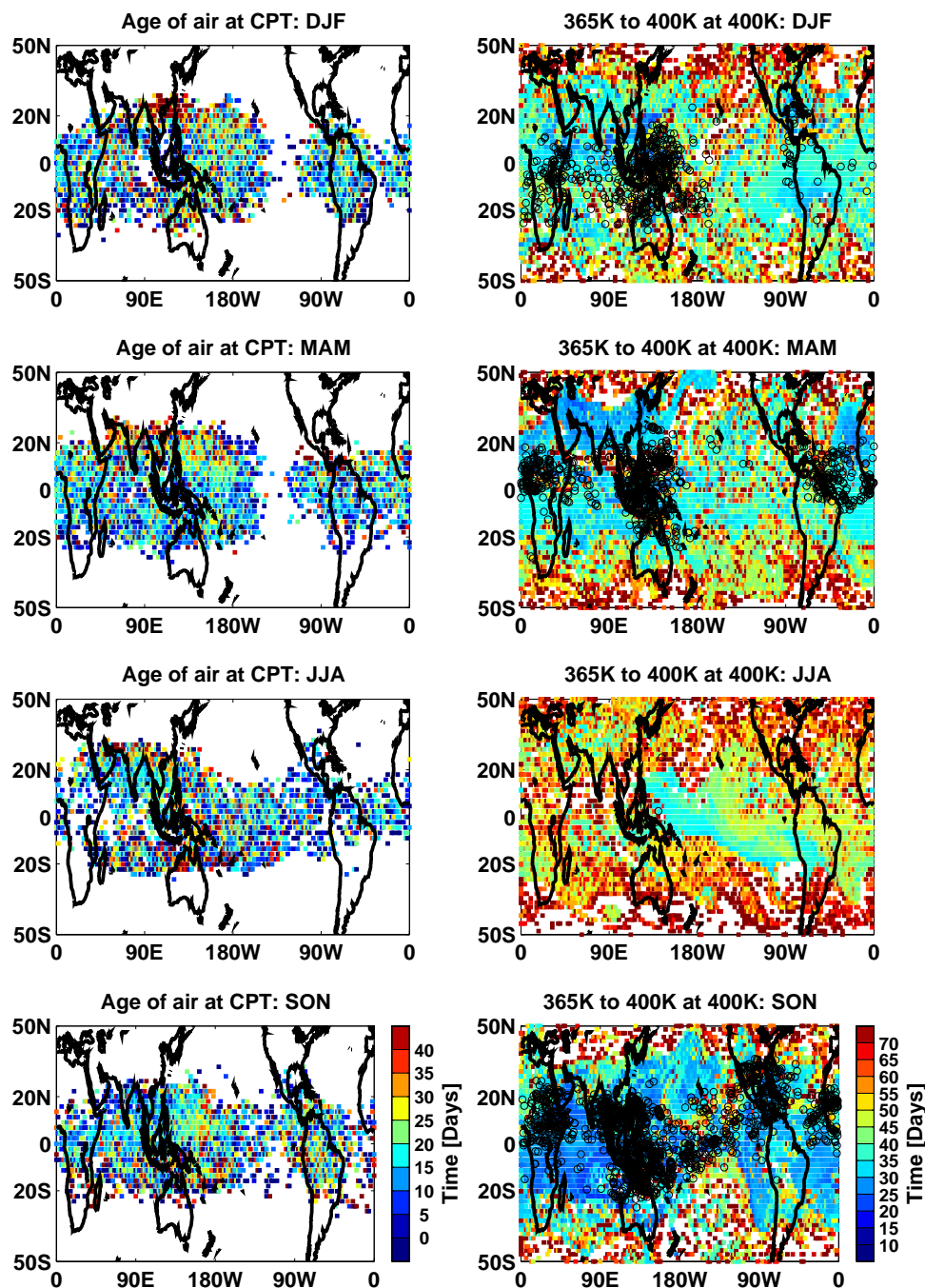


Fig. 6. Map of effective age of the air reaching the CPT at the CPT (left panels) for trajectories traversing the TTL in 2000 for all seasons. The right hand panels display the residence times from 365 K to 400 K at 400 K. The black open circles in the right-hand panels display the trajectory locations at 355 K if the residence times 365–400 K are shorter than 30 days.

Between a quarter and a third of all the back-trajectories started at 400 K between 50° N and 50° S fail to run back to 365 K after 3 months. The uppermost panels of Fig. 7 show few of the trajectories reaching 400 K originate from 365 K north of 30° N in DJF and similarly few south of 30° S in JJA – following the ITCZ latitudinal TTL entry shift with sea-

son (Fueglistaler et al., 2009). CPTs crossings are only seen between 20° N and 20° S irrespective of season. Figure 7 displays the narrow latitude band associated with the CPTs for TTL transport (middle panels), the latitude ranges before (top panels) and after (bottom panels) being much broader.

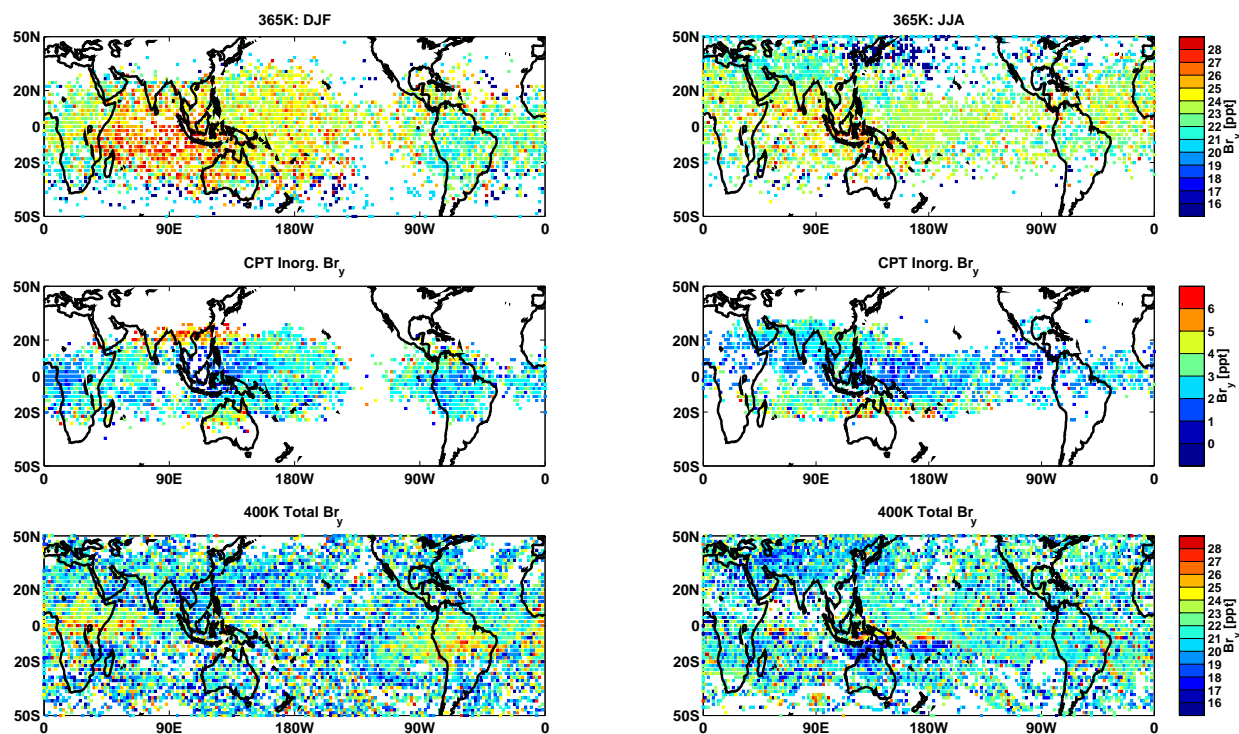


Fig. 7. Br_y transport across the TTL for DJF and JJA. Top row provides the spatial distribution of total Br_y ($\text{Br}_y^{\text{Inorg}} + \text{Br}_y^{\text{OrgSL}}$) at $\Theta = 365$ K – i.e. the convective influence before this level. The second row displays inorganic Br_y at the cold point available to washout. The third row gives the spatial distribution of total Br_y at $\Theta = 400$ K.

The trajectories used in this study were driven by clear-sky radiative heating rates. We explored the sensitivity of our results to all-sky radiative heating rates and found negligible differences despite the warmer CPTs and shorter residence times below 370 K. An increase of ~ 0.5 ppt Br_y was found across all runs, mainly due to the altered initialization process.

3.2 The role of organic bromine emissions

The effect of altering the underlying concentrations of the SLS detrained into the TTL with convection from the two scenarios supplied in Table 2 is displayed in Fig. 9. The emission scenario based upon Kerkweg et al. (2008) increases CH₃Br and reduces the concentrations of CHBr₃ and CH₂Br₂ from coastal and oceanic sources relative to the scenario of Yokouchi et al. (2005). The lifetime of CH₃Br is also increased from 0.7 to 1.0 yr consistent with the work of Montzka et al. (2003) and Kerkweg et al. (2008); which suggest a lifetime of $\gg 0.8$ and 1 yr, respectively. Such a shift to longer lived species reduces the importance of convection and reduces the magnitude of the seasonality (though it is still evident). The median Br_y arriving at 400 K, is reduced from 21.3 ppt to 20.3 ppt (VLSL 4.8 to 3.8 ppt) and the distribution is considerably narrowed by changing the underlying

emission sources and lifetime. However, these different BL emission scenarios have a much smaller impact on stratospheric Br_y than one might have expected. This is because the free tropospheric fraction constitutes 0.7 or more of convective entrainment (Romps and Kuang, 2010) and thereby is a constant VLSL concentration independent of location, strongly attenuating the impact of source strength and geographical patterns. No claim is made here that the assumption of a single typical free tropospheric VLSL concentration is valid. Rather, the assumption is made only because of lack of measurements of the global distribution of VLSL in the free troposphere. Our result highlights the need for more measurements and to focus future model studies on the FT mixing component of the system, to better constrain how FT VLSL concentrations are influenced by BL emissions.

Recent modelling combined with measurements studies have investigated the contribution of the bromine VLSL of bromoform (CHBr₃) and dibromomethane (CH₂Br₂) (Sinnhuber and Folkins, 2006; Laube et al., 2008; Aschmann et al., 2009; Gettelman et al., 2009; Hossaini et al., 2010; Liang et al., 2010) upon the stratospheric Br_y budget. As Fig. 2 shows these two species are the dominant among the bromine VLSLs, but CHBr₂Cl may also be important. The most abundant bromine containing substance – CH₃Br, due to its lifetime being short enough relative to the TTL

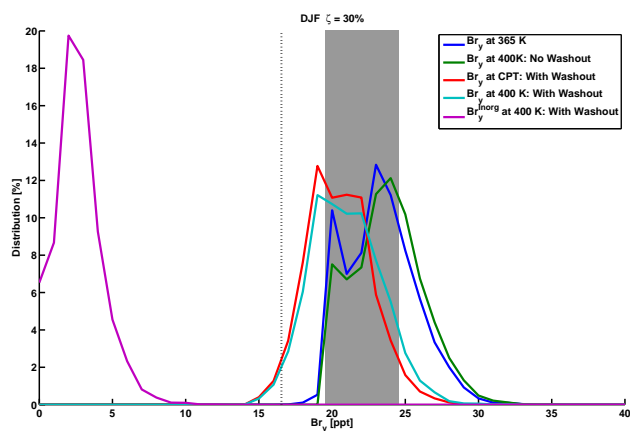


Fig. 8. The breakdown of the Br_y distribution over all trajectories (% of total trajectories). Br_y at $\Theta=365$ K (blue), at $\Theta=400$ K for complete washout ($\gamma=1$) (teal), at $\Theta=400$ K with no washout ($\gamma=0$) (green), and at the CPT directly after complete washout $\gamma=1$ (red) (this is the same as the distribution at $\Theta=400$ K when no convection above the CPT is assumed). The total Br_y^{Inorg} at 400 K is also provided (magenta). The dashed line provides the Halons + CH₃Br contribution (16.5 ppt for 2000), and the grey shaded region the WMO recommendation for an additional 3–8 ppt from VLSL (WMO, 2006, Table 2–8).

residence times and its source fluctuations, also needs to be taken into account in SLS studies attempting to reconcile the stratospheric Br_y budget.

3.3 The role of convection

Br_y transport across the TTL for DJF and JJA is displayed spatially in Fig. 7 for a convective efficiency $\zeta=30\%$ and quantitatively in Figs. 8–10.

The difference between the blue and green curves of Fig. 8 illustrates the effect of convection in DJF above 365 K on Br_y with no washout and $\zeta=30\%$, shifting the distribution peak by 1–2 ppt (note the loss of the initialization peak at 21 ppt). When complete washout is considered, the convective influence after the CPT – given by the difference between red and teal curves – is small (0.4 ppt difference in median values). This finding is in line with the findings of Aschmann et al. (2009), who found negligible change when convection above 380 K was switched off.

Figure 9 shows that for a convective efficiency ζ of 30% in DJF (“Standard”), the VLSLs that reaches 400 K has a median value of 4.8 ppt. This is lower than the 6–7 ppt tropical maximum modelled by Warwick et al. (2006) with a more complex emission pattern than the simple high source concentrations for ocean and coastal areas used here.

Changing the BL component of detrained air from 10% to 50% broadens of the Br_y distribution reaching 400 K and increases the median value from 19.6 ppt to 22.9 ppt (VLSL 3.1 ppt to 6.4 ppt), with a distribution spanning the higher end

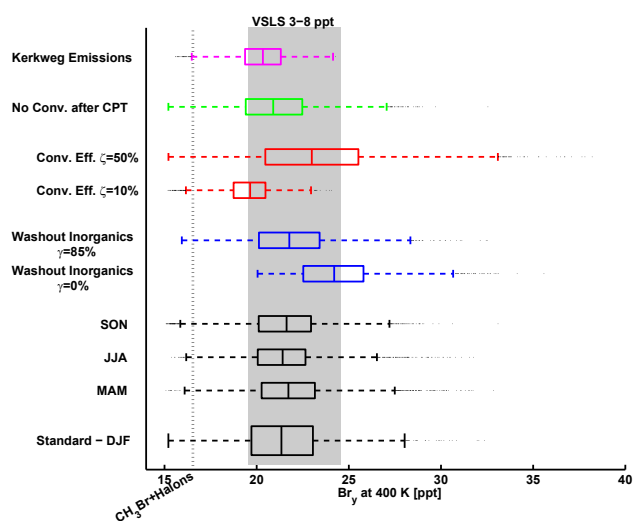


Fig. 9. Boxplots illustrating the different distributions of Br_y arriving at 400 K from all trajectories traversing the TTL in 2000. The boxes illustrate the 25-th to 75-th percentiles, the whiskers 1.5× the interquartile range and the crosses outliers. Unless otherwise stated the distributions are for DJF, using Yokouchi et al. (2005) boundary layer concentrations, a 30% BL component to the convective outflow, and washout at the CPT of 100%. The lowermost bar is this standard case, and all other bars show the sensitivity to the resultant Br_y for the indicated change. The dashed line provides the Halons + CH₃Br contribution for 2000 (WMO, 2006, Table 8–5) and the grey shaded region the WMO recommendation for an additional VLSL contribution of 3–8 ppt (WMO, 2006, Table 2–8).

of the required additional 8 ppt inferred from BrO measurements (Law and Sturges, 2007). A 50% BL component of the convective outflow, however, is not supported by the study of Romps and Kuang (2010). Changing the BL component from 10% to 30% increases Br_y from 19.6 ppt to 21.3 ppt (VLSL 3.1 ppt to 4.8 ppt), showing this is a key sensitivity.

3.4 Role of CPT washout

The Br_y^{Inorg} available for washout is displayed in the middle panels of Fig. 7. In Fig. 8 the role of washout is seen as the difference between the green and teal curves. From Fig. 9 washout reduces the Br_y that would arrive at 400 K from 24.2 to 21.3 ppt (VLSL 7.7 ppt to 4.8 ppt). Thus washout removes 38% of the Br_y at the CPT, this is (not surprisingly) lower than the 50% found by Aschmann et al. (2009) who consider only the most short-lived substance CHBr₃.

Complete retention of inorganic bromine results in a stratospheric Br_y concentration distribution consistent only with observations at the higher end of the range of stratospheric BrO observations (Sinnhuber et al., 2002, 2005; Schofield et al., 2004, 2006; Salawitch et al., 2005; Dorf et al., 2006; Livesey et al., 2006; Hendrick et al., 2007; Theys et al., 2009). We expect that washout is effective – with HOBr and HBr being very soluble species constituting 85%

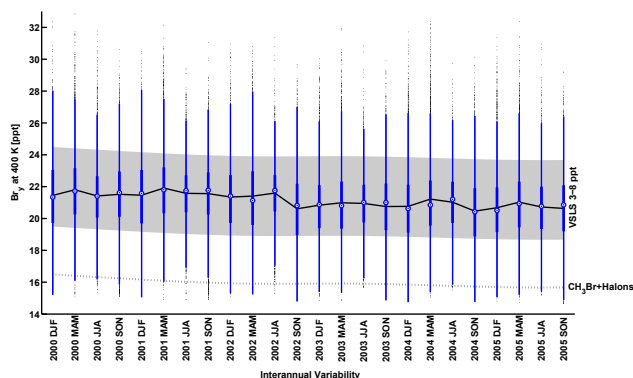


Fig. 10. Boxplots displaying the variability of the distributions of Br_y arriving at 400 K from all trajectories traversing the TTL from 2000 to 2005. The boxes illustrate the 25-th to 75-th percentiles, the whiskers 1.5× the interquartile range and the crosses outliers. Yokouchi et al. (2005) boundary layer concentrations, a 30% BL component to the convective outflow, and washout at the CPT of 100% are used. The mean values for each year are given by the solid black line. The dashed line provides the Halons + CH₃Br contribution (with the prescribed decreasing trend) (WMO, 2006, Table 8–5) and the grey shaded region the WMO recommendation for an additional VLSLs contribution of 3–8 ppt (WMO, 2006, Table 2–8).

of the Br_y^{Inorg} in the TTL (Fig. 4 from Yang et al., 2005). If we assume a 15% retention of PGs, this would result in 0.5 ppt more Br_y arriving at 400 K, this would be indistinguishable from increased source concentrations or a slight increase in BL to TTL convective efficiency. In contrast, a new study of Aschmann et al. (2011) shows the uptake of HBr upon ice to be ineffective, therefore the washout efficiency is close to 0. If no washout occurs as concluded by Aschmann et al. (2011) then the BL component of the detrained air must be less than about 0.3 to remain consistent with stratospheric BrO measurements. Thus illustrating that the uncertainty in the washout process remains a key sensitivity in the stratospheric Br_y budget.

As there is little seasonality in the ERA-Interim detrainment rates and no seasonality in the sources in this study, the seasonality seen in Fig. 9 arises from washout timing (residence times) and ITCZ seasonal shift in the TTL transport (as found also in the study of Liang et al., 2010). Washout is most effective in DJF with a mean loss of 2.9 ppt, and least effective in JJA with only 2.4 ppt loss, (MAM and SON having mean losses 2.4 ppt and 2.5 ppt, respectively). Under no washout (i.e. purely ITCZ driven), DJF and MAM receive mean Br_y concentrations of 24.2 ppt, this is followed by SON with 24.1 ppt and JJA with 23.8 ppt. Therefore, the resultant seasonality is complicated: DJF, while receiving more convective injection of Br_y succumbs to higher washout, exactly opposite to JJA where less convective injection of Br_y occurs and less washout. Thereby washout at the CPT acts to dampen any convectively introduced seasonality. The sea-

sonality in Figs. 9 and 10 displays this complicated, almost flat behavior. The tape-recorder seasonality seen by the similar model study of Aschmann et al. (2009) in soluble Br_y above the CPT with a maxima in boreal summer reveals a difference that is best addressed with an observational seasonal study. We find little seasonality in inorganic Br_y with mean values of 3.1 ppt: 15% of the total Br_y at 400 K, for all seasons except SON where it is only 2.3 ppt (11%).

4 Conclusions

With this conceptual study, we have been able to explore the sensitivity of Br_y arriving at 400 K due to emission sources, convection and washout. We conclude:

- Longer-lived bromine source gases result in narrower Br_y distributions at 400 K. Determining the TTL OH field will be vital in constraining the TTL lifetimes of the SLS, and therefore determining the source importance.
- The delivery of short-lived substances to the TTL is critically dependent upon the convective detrainment rates which are very difficult to verify. Future studies that look at the seasonality in convective detrainment will aid in reducing this current uncertainty.
- The efficiency with which boundary layer organic Br_y source gases are delivered to the convective outflow is very important – 1.7 ppt additional Br_y results as the efficiency is increased from 10 to 30% (the expected range from Roms and Kuang, 2010).
- With the chemical composition of the convective outflow being dominated by that of in-mixed free tropospheric air, the stratospheric Br_y budget is critically affected by the processes that control the free tropospheric VLSLs, in particular, to what extent the geographic distributions of free tropospheric VLSLs are controlled by large-scale transport versus local emissions.
- We find that the seasonal migration of the ITCZ and the seasonal cycle in residence time both produce a corresponding seasonality in Br_y delivery to the stratosphere, but that the two cycles are out of phase and hence largely cancel. A larger seasonality of stratospheric Br_y may be expected if deep convective outflow would have a substantial seasonality. This seasonality however would be expected to be dampened if the washout displays a higher efficiency at colder temperatures.
- Deep convection perturbing an air mass after the last washout event plays only a minor role in Br_y arriving at 400 K (0.4 ppt). However, increased sensitivities are achieved with higher boundary layer VLSLs concentrations or a higher boundary layer component of the convective outflow.

- No washout of Br_y^{Inorg} at the cold point results in a distribution that is at the higher end of inferences of Br_y from stratospheric BrO measurements. Complete washout removes 2.4–2.9 ppt, therefore establishing the effectiveness of washout is crucial in reducing the uncertainty in the stratospheric Br_y budget.

Convective dilution determines the significance of emissions in the stratospheric Br_y budget, therefore obtaining accurate spatial and temporal free tropospheric source gas concentrations will aid future studies. Another source of uncertainty is the assumption that the free troposphere delivers no product gases: is this a reasonable assumption given the well-mixed nature and high moisture situation, or could product gases be expected to be delivered with convective ice lofting?

Despite the simplistic nature and coarse assumptions made in this study, the widths of the Br_y distributions arriving 400 K are narrower than the range of 3–8 ppt derived from BrO measurements (Law and Sturges, 2007). Improvement in our observational knowledge of the total stratospheric Br_y (i.e. reducing the current VLSL 3–8 ppt uncertainty range) will significantly aid in modelling stratospheric Br_y, and making long term stratospheric ozone projections. Establishing emission sources, bromine source gas TTL lifetimes, the amount of boundary layer air within convective outflow and the efficiency of the washout process are the areas which require better constraints in refining the the Br_y budget. The convective detrainment rates are a vital component of this system, observational support for convective strength and seasonality will improve our ability to accurately model the stratospheric Br_y budget.

Acknowledgements. We thank I. Folkins for useful discussions and the 4 anonymous reviewers and Björn-Martin Sinnhuber for their helpful suggestions in improving this manuscript. The authors thank ECMWF for providing ERA-Interim data via special project DERESI. Funding support for this work was provided by the European Union (EU) funded WaVES (MIF1-CT-2006-039646), SCOUT-O3 (GOCE-CT-2004-505390) and SHIVA (SHIVA-226224-FP7-ENV-2008-1) projects.

Edited by: P. Haynes

References

- Andreae, M. O., Atlas, E., Harris, G. W., Helas, G., deKock, A., Koppmann, R., Maenhaut, W., Manø, S., Pollock, W. H., Rudolph, J., Scharffe, D., Schebeske, G., and Welling, M.: Methyl halide emissions from savanna fires in southern Africa, *J. Geophys. Res.*, 101, D19, 23603–23613, 1996.
- Aschmann, J., Sinnhuber, B. M., Atlas, E. L., and Schauffler, S. M.: Modeling the transport of very short-lived substances into the tropical upper troposphere and lower stratosphere, *Atmos. Chem. Phys.*, 9, 23, 9237–9247, doi:10.5194/acp-9-9237-2009, 2009.
- Aschmann, J., Sinnhuber, B. M., Chipperfield, M. P., and Hossaini, R.: Impact of deep convection and dehydration on bromine loading in the upper troposphere and lower stratosphere, *Atmos. Chem. Phys. Discuss.*, 11, 121–162, doi:10.5194/acpd-11-121-2011, 2011.
- Carpenter, L. J., Jones, C. E., Dunk, R. M., Hornsby, K. E., and Woeltjen, J.: Air-sea fluxes of biogenic bromine from the tropical and North Atlantic Ocean, *Atmos. Chem. Phys.*, 9, 1805–1816, doi:10.5194/acp-10-4611-2010, 2009.
- Dessler, A. E.: The effect of deep, tropical convection on the tropical tropopause layer, *J. Geophys. Res.*, 107(D3), 4033, doi:10.1029/2001JD000511, 2002.
- Dessler, A. E., Hanisco, T. F., and Fueglistaler, S.: Effects of convective ice lofting on H₂O and HDO in the tropical tropopause layer, *J. Geophys. Res.*, 112, D18309, doi:10.1029/2007JD008609, 2007.
- Dorf, M., Butler, J. H., Butz, A., Camy-Peyret, C., Chipperfield, M. P., Kritten, L., Montzka, S. A., Simmes, B., Weidner, F., and Pfeilsticker, K.: Long-term observations of stratospheric bromine reveal slow down in growth, *Geophys. Res. Lett.*, 33, L24803, doi:10.1029/2006gl027714, 2006.
- Dvortsov, V. L., Geller, M. A., Solomon, S., Schauffler, S. M., Atlas, E. L., and Blake, D. R.: Rethinking reactive halogen budgets in the midlatitude lower stratosphere, *Geophys. Res. Lett.*, 26, 1699–1702, 1999.
- ECMWF: Integrated forecast system CY33r1 Documentation, Part IV: Physical Processes, chap. 5: Convection, p. 69, <http://www.ecmwf.int/research/ifsdocs/CY33r1/index.html>, 2008.
- Folkins, I., Bernath, P., Boone, C., Lesins, G., Livesey, N., Thompson, A. M., Walker, K., and Witte, J. C.: Seasonal cycles of O-3, CO, and convective outflow at the tropical tropopause, *Geophys. Res. Lett.*, 33, L16802, doi:10.1029/2006GL026602, 2006.
- Fueglistaler, S., Wernli, H., and Peter, T.: Tropical troposphere-to-stratosphere transport inferred from trajectory calculations, *J. Geophys. Res.*, 109, D03108, doi:10.1029/2003JD004069, 2004.
- Fueglistaler, S., Dessler, A. E., Dunkerton, T. J., Folkins, I., Fu, Q., and Mote, P. W.: Tropical Tropopause Layer, *Rev. Geophys.*, 47, RG1004, doi:10.1029/2008rg000267, 2009.
- Gottelman, A., Lauritzen, P. H., Park, M., and Kay, J. E.: Processes regulating short-lived species in the tropical tropopause layer, *J. Geophys. Res.*, 114, D13303, doi:10.1029/2009jd011785, 2009.
- Hendrick, F., Van Roozendaal, M., Chipperfield, M. P., Dorf, M., Goutail, F., Yang, X., Fayt, C., Hermans, C., Pfeilsticker, K., Pommereau, J. P., Pyle, J. A., Theys, N., and De Mazière, M.: Retrieval of stratospheric and tropospheric BrO profiles and columns using ground-based zenith-sky DOAS observations at Harestua, 60 degrees N, *Atmos. Chem. Phys.*, 7, 18, 4869–4885, doi:10.5194/acp-7-4869-2007, 2007.
- Hoskins, B. J.: Towards a PV-Theta view of the general-circulation, *Tellus*, 43, 4, 27–35, 1991.
- Hossaini, R., Chipperfield, M. P., Monge-Sanz, B. M., Richards, N. A. D., Atlas, E., and Blake, D. R.: Bromoform and dibromomethane in the tropics: a 3-D model study of chemistry and transport, *Atmos. Chem. Phys.*, 10, 2, 719–735, doi:10.5194/acp-10-719-2010, 2010.
- James, R., Bonazzola, M., Legras, B., Surbled, K., and Fueglistaler, S.: Water vapor transport and dehydration above convective outflow during Asian monsoon, *Geophys. Res. Lett.*, 35, L20810, doi:10.1029/2008GL035441, 2008.

- Kerkweg, A., Jöckel, P., Warwick, N., Gebhardt, S., Brenninkmeijer, C. A. M., and Lelieveld, J.: Consistent simulation of bromine chemistry from the marine boundary layer to the stratosphere – Part 2: Bromocarbons, *Atmos. Chem. Phys.*, 8, 19, 5919–5939, doi:10.5194/acp-8-5919-2008, 2008.
- Laube, J. C., Engel, A., Bönisch, H. and Mobius, T., Worton, D. R., Sturges, W. T., Grunow, K., and Schmidt, U.: Contribution of very short-lived organic substances to stratospheric chlorine and bromine in the tropics – a case study, *Atmos. Chem. Phys.*, 8, 23, 7325–7334, doi:10.5194/acp-8-7325-2008, 2008.
- Law, K. S. and Sturges, W. T.: Halogenated very short-lived substances, chap. 2, 572 pp., World Meteorological Organization, Geneva, Switzerland, 2007.
- Lee, A. M., Jones, R. L., Kilbane-Dawe, I., and Pyle, J. A.: Diagnosing ozone loss in the extratropical lower stratosphere, *J. Geophys. Res.*, 107, D11, 4110, doi:10.1029/2001JD000538, 2002.
- Liang, Q., Stolarski, R. S., Kawa, S. R., Nielsen, J. E., Douglass, A. R., Rodriguez, J. M., Blake, D. R., Atlas, E. L., and Ott, L. E.: Finding the missing stratospheric Br_y: a global modeling study of CHBr₃ and CH₂Br₂, *Atmos. Chem. Phys.*, 10, 5, 2269–2286, doi:10.5194/acp-10-2269-2010, 2010.
- Livesey, N. J., Kovalenko, L. J., Salawitch, R. J., MacKenzie, I. A., Chipperfield, M. P., Read, W. G., Jarnot, R. F., and Waters, J. W.: EOS Microwave Limb Sounder observations of upper stratospheric BrO: Implications for total bromine, *Geophys. Res. Lett.*, 33, L20817, doi:10.1029/2006gl026930, 2006.
- Montzka, S. A., Butler, J. H., Hall, B. D., Mondeel, D. J., and Elkins, J. W.: A decline in tropospheric organic bromine, *Geophys. Res. Lett.*, 30, 15, 1826, doi:10.1029/2003gl017745, 2003.
- Romps, D. M. and Kuang, Z. M.: Do Undiluted Convective Plumes Exist in the Upper Tropical Troposphere?, *J. Atmos. Sci.*, 67(2), 468–484, doi:10.1175/2009jas3184.1, 2010.
- Salawitch, R. J., Weisenstein, D. K., Kovalenko, L. J., Sioris, C. E., Wennberg, P. O., Chance, K., Ko, M. K. W., and McLinden, C. A.: Sensitivity of ozone to bromine in the lower stratosphere, *Geophys. Res. Lett.*, 32, L05811, doi:10.1029/2004GL021504, 2005.
- Schofield, R., Kreher, K., Connor, B. J., Johnston, P., Thomas, A., Shooter, D., Chipperfield, M., Rodgers, C. D., and Mount, G.: Retrieved tropospheric and stratospheric BrO columns over Lauder, New Zealand, *J. Geophys. Res.*, 109, D14304, doi:10.1029/2003JD004463, 2004.
- Schofield, R., Johnston, P. V., Thomas, A., Kreher, K., Connor, B. J., Wood, S., Shooter, D., Chipperfield, M. P., Richter, A., von Glasow, R., and Rodgers, C. D.: Tropospheric and stratospheric BrO columns over Arrival Heights, Antarctica, 2002, *J. Geophys. Res.*, 111, D22310, doi:10.1029/2005JD007022, 2006.
- Simmons, A. J., Uppala, S., Dee, D., and Kobayashi, S.: ERA Interim: New ECMWF reanalysis products from 1989 onwards, *ECMWF Newsl.*, 110, 25–35, 2007.
- Sinnhuber, B. M. and Folkins, I.: Estimating the contribution of bromoform to stratospheric bromine and its relation to dehydration in the tropical tropopause layer, *Atmos. Chem. Phys.*, 6, 4755–4761, doi:10.5194/acp-6-4755-2006, 2006.
- Sinnhuber, B. M., Arlander, D. W., Bovensmann, H., Burrows, J. P., Chipperfield, M. P., Enell, C. F., Frieß, U., Hendrick, F., Johnston, P. V., Jones, R. L., Kreher, K., Mohamed-Tahrin, N., Müller, R., Pfeilsticker, K., Platt, U., Pommereau, J. P., Pundt, I., Richter, A., South, A., Tørnkvist, K. K., Van Roozendaal, M., Wagner, T., and Wittrock, F.: Comparison of measurements and model calculations of stratospheric bromine monoxide, *J. Geophys. Res.*, 107(D19), 4398, doi:10.1029/2001JD000940, 2002.
- Sinnhuber, B. M., Rozanov, A., Sheode, N., Afe, O. T., Richter, A., Sinnhuber, M., Wittrock, F., Burrows, J. P., Stiller, G. P., von Clarmann, T., and Linden, A.: Global observations of stratospheric bromine monoxide from SCIAMACHY, *Geophys. Res. Lett.*, 32, L20810, doi:10.1029/2005GL023839, 2005.
- Sioris, C. E., Kovalenko, L. J., McLinden, C. A., Salawitch, R. J., Van Roozendaal, M., Goutail, F., Dorf, M., Pfeilsticker, K., Chance, K., von Savigny, C., Liu, X., Kurosu, T. P., Pommereau, J. P., Bosch, H., and Frerick, J.: Latitudinal and vertical distribution of bromine monoxide in the lower stratosphere from Scanning Imaging Absorption Spectrometer for Atmospheric Cartography limb scattering measurements, *J. Geophys. Res.*, 111, D14301, doi:10.1029/2005jd006479, 2006.
- Theys, N., Van Roozendaal, M., Errera, Q., Hendrick, F., Daerden, F., Chabrillat, S., Dorf, M., Pfeilsticker, K., Rozanov, A., Lotz, W., Burrows, J. P., Lambert, J. C., Goutail, F., Roscoe, H. K., and De Mazière, M.: A global stratospheric bromine monoxide climatology based on the BASCOE chemical transport model, *Atmos. Chem. Phys.*, 9(3), 831–848, doi:10.5194/acp-9-831-2009, 2009.
- Tost, H., Lawrence, M. G., Brühl, C., Jöckel, P., Team, G., and Team, S.-O.-D. A.: Uncertainties in atmospheric chemistry modelling due to convection parameterisations and subsequent scavenging, *Atmos. Chem. Phys.*, 10, 4, 1931–1951, doi:10.5194/acp-10-1931-2010, 2010.
- von Glasow, R., von Kuhlmann, R., Lawrence, M. G., Platt, U., and Crutzen, P. J.: Impact of reactive bromine chemistry in the troposphere, *Atmos. Chem. Phys.*, 4, 2481–2497, doi:10.5194/acp-4-2481-2004, 2004.
- Warwick, N. J., Pyle, J. A., Carver, G. D., Yang, X., Savage, N. H., O'Connor, F. M., and Cox, R. A.: Global modeling of biogenic bromocarbons, *J. Geophys. Res.*, 111, D24305, doi:10.1029/2006jd007264, 2006.
- WMO: Scientific assessment of ozone depletion, 2006 : report of the Montreal Protocol Scientific Assessment Panel, Tech. rep., WMO Global Ozone Research and Monitoring Project – Report No. 50, 2006.
- Wofsy, S. C., McElroy, M. B., and Yung, Y. L.: The Chemistry of Atmospheric Bromine, *Geophys. Res. Lett.*, 2, 215–218, 1975.
- Wohlmann, I. and Rex, M.: Improvement of vertical and residual velocities in pressure or hybrid sigma-pressure coordinates in analysis data in the stratosphere, *Atmos. Chem. Phys.*, 8, 2, 265–272, doi:10.5194/acp-8-265-2008, 2008.
- Yang, X., Cox, R. A., Warwick, N. J., Pyle, J. A., Carver, G. D., O'Connor, F. M., and Savage, N. H.: Tropospheric bromine chemistry and its impacts on ozone: A model study, *J. Geophys. Res.*, 110, D23311, doi:10.1029/2005jd006244, 2005.
- Yokouchi, Y., Hasebe, F., Fujiwara, M., Takashima, H., Shiotani, M., Nishi, N., Kanaya, Y., Hashimoto, S., Fraser, P., Toom-Saunty, D., Mukai, H., and Nojiri, Y.: Correlations and emission ratios among bromoform, dibromochloromethane, and dibromomethane in the atmosphere, *J. Geophys. Res.*, 110, D23309, doi:10.1029/2005jd006303, 2005.